Available online at www.sciencedirect.com

ScienceDirect

IFAC Papers Online CONFERENCE PAPER ARCHIVE

IFAC-PapersOnLine 48-1 (2015) 447–452

# Development and analysis of a mathematical model for a synthetic biological cell

**Eugenia Schneider** * **Michael Mangold** **

* *Max-Planck-Institute for Dynamics of Complex Technical Systems, 39106 Magdeburg, Germany (e-mail: eschneider@mpi-magdeburg.mpg.de)*

** *Max-Planck-Institute for Dynamics of Complex Technical Systems, 39106 Magdeburg, Germany (e-mail: mangold@mpi-magdeburg.mpg.de)*

**Abstract:** Synthetic biology as a new discipline is driven by progresses made in the understanding of microbiological processes and its mathematical description by system biological models. The topic of synthetic biology is a systematic construction of artificial biological systems with tailored properties. The subject of this work is to develop an artificial cell model consisting of functional biological devices like genome, transcriptome, proteome, metabolome, with a structure that guarantees a synchronization of the devices in a robust way. The mathematical model shown in this work involves the metabolism, the polymerization subsystem and the membrane. The model structure enables an oscillatory behavior of the system with a stable limit cycle. Also the system provides a robust self-replicating state and a biological robustness with respect to parameter uncertainties.



*Keywords:* nonlinear systems, simulation, synthetic biology, protocell, biocybernetics

## 1. INTRODUCTION

Enormous progresses have been made in the fields of microbiology and systems biology. The mathematical modeling of biological systems is becoming increasingly important for a deepened understanding of intracellular processes. Synthetic biology as a new biological field aims at the systematic construction of artificial biological systems with tailored properties. Two main working directions can be identified in synthetic biology: the top-down and the bottom-up approach. The top down approach starts from an existing micro-organism whose genome is manipulated and reduced intentionally based on acquired knowledge and hoping to achieve a desired property(Keasling, 2012; Jaschke et al., 2012). In contrast, the bottom up approach starts on the molecular level from functional biological devices like genome, transcriptome, proteome, metabolome and attempts to assemble these biological parts into an artificial cell (Stano, 2011; Pohorille and Deamer, 2002). The idea behind the bottom-up approach is to obtain better understanding and improved predictability by building up something from zero. In reality, the bottom-up approach still has to solve many problems before reaching the final goal of a self-reproducing artificial cell.

In spite of existing mathematical models, which have been developed for describing artificial cells (Gánti, 2003; Novák and Tyson, 2008), there is a need for further theoretical analysis and mathematical modeling for a deepened insights into functional device interactions. Various qualitative artificial cell models have been proposed during the last decades (Gánti, 2003; Novák and Tyson, 2008; Rasmussen et al., 2003). As pointed out by Rasmussen et al. most of these models may be structured into three functional devices: a container forming the boundary of the cell, a metabolism generating the building blocks of the cell, and a programming part containing genetic information and regulating the processes inside the cell (Rasmussen et al., 2003).

The issue of this work is the definition of a structure that masters the synchronization of those three devices. The synchronization problem includes the question of robust functional dependence of the devices in the sense that the material in each of the devices has at least doubled at the end of the cell cycle. In such a case we can assume that self-replication of the artificial cell is achieved. The demand for the biological robustness of the model, i.e. a certain independence of the qualitative system behavior on the kinetic parameter values, is justified by the aim to being able to deal with perturbations.

The dependence of the functional devices is well exemplified by the Chemoton model described by T. Gánti (Gánti, 2003). The Chemoton comprises three functional self-reproducing devices. The autocatalytic chemical cycle can be seen as the metabolic cycle and produces precursor molecules needed for reproducing the other two devices. One precursor is consumed as a monomer by the template polymerization subsystem which serves as an information carrier. The second precursor reacts with a by-product of the polymerization cycle into a membrane molecule. The membrane represents a container and grows proportional to the production of the polymerization by-product un-


10.1016/j.ifacol.2015.05.018

til the volume of the Chemoton is duplicated. Then the division of the protocell occurs spontaneously.

It was shown by the simulation studies of Csendes (1984) that the Chemoton model displays self-sustained oscillations. This behavior could be verified by our own simulations (data not shown). However, if we wanted to reduce the complexity of the model structure these oscillations were not necessarily synchronized with cell growth, i.e. the time needed to double the total amount of material in the cell is not always an integer multiple of the oscillation's period.

The task of this work is to find a model structure with less complexity in comparison to the Chemoton and with an inherent mechanism guaranteeing the synchronization of container, metabolism and program for a wide range of kinetic parameter values. The minimal cascade model for the mitotic oscillator described by Goldbeter (1991) (Fig.1) provides such a model structure, which we have used as a starting point for the design of a new artificial cell model.

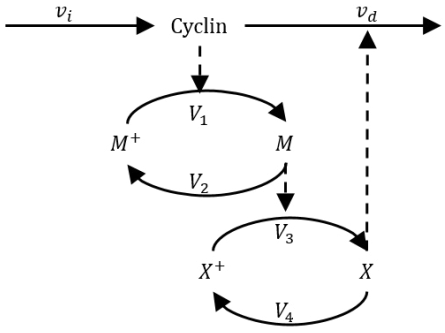


Fig. 1. Minimal cascade model for mitotic oscillations. (Goldbeter, 1991)

## 2. ARTIFICIAL CELL MODEL

By combining the functional devices as proposed in the Chemoton model with the less complex structure of Goldbeter's minimal cascade we developed a model of a self-reproducible artificial cell. Fig.2 shows a scheme of this model representing the mother cell ($S_1$) and the daughter cell ($S_2$).

Three main functional devices form the mother cell: the metabolism ($A$), the polymerization subsystem ($P_t$, $P$) and the membrane ($M^*$, $M$). The activity of metabolism $A$ is induced by the polymer template $P_t$ with a constant rate $v_A$ and hence slows down towards the end of the polymer replication when there is hardly $P_t$ in the cell. $A$ catalyzes the polymer replication until $P_t$ is completely consumed. The replicated polymer splits into the polymer template $P_t$ and the new polymer $P_{t,d}$. During the polymerization the new growing polymer $P$ catalyzes the conversion of catalytically inactive membrane building blocks $M^*$ into the active state $M$. $M$ triggers the transformation of $A$, $P$ and $M$ to daughter cell components $A_d$, $P_{t,d}$, $M_d^*$ with constant degradation rates $v_{dA}$, $v_{dP}$ and $v_{dM}$. This initiates the cell division in our model.

The proposed structure establishes a close interaction between the activation of the metabolism and the replication

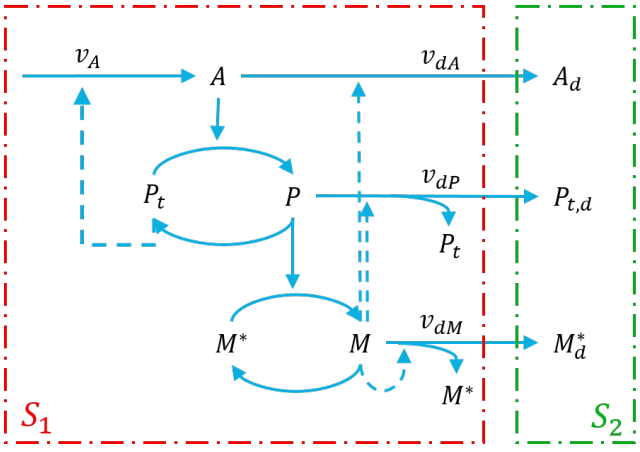


Fig. 2. Artificial cell model based on Goldbeter's minimal cascade including the functional devices of Gánti's Chemoton. System $S_1$ represents the mother cell including the metabolism $A$, the polymer template $P_t$, the new growing polymer $P$, catalytically inactive membrane building blocks $M^*$ and catalytically active membrane building blocks $M$. System $S_2$ represents the daughter cell arising from degraded mother cell components. The daughter cell contains initially the metabolism component $A_d$, the polymer template $P_{t,d}$ and the membrane composed of inactive membrane building blocks $M_d^*$. Arrows symbolize catalysis (→) and induction (⇢).

of the polymer. This interaction forces a synchronization between metabolism and polymerization. In addition, the membrane subsystem serves as a self-replicating unit (Fig.3). First an inactive membrane building block becomes active catalyzed by a polymer. Then a second active membrane building block binds the first one and induces its duplication. After the copying process the inducing $M$ molecule is free and able to induce another replication cycle. The newly generated $M$ molecules become inactive during the separation of the daughter cell.

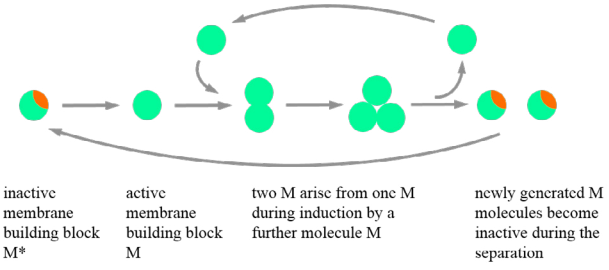


Fig. 3. Self-replication of membrane building blocks.

In the first instance, we assume that newly generated membrane building blocks $M$ remain inside the mother cell, so the volume changes of the mother cell are neglected.

### *2.1 Model equations*

The proposed model system possesses three different operation modes, which may be represented as a Petri net with three nodes, as illustrated in Fig.4.

First, we assume that the total quantity of the polymer template $P_t$ and the newly synthesized polymer $P$ is $P_t$ +

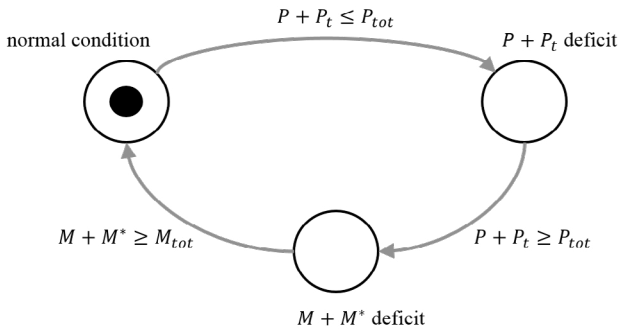


Fig. 4. Representation of the protocell's three operation modes as a Petri net.

$P = P_{tot}$ and the total concentration of inactive and active membrane building blocks amounts to $M^* + M = M_{tot}$. We call this case *normal condition* (Fig.4). Under normal conditions, the following chemical reactions take place inside the protocell:

$$\xrightarrow[v_A]{P_t} \mathrm{A} \tag{1}$$

$$\mathrm{P_t} \xrightarrow[k_1]{A} \mathrm{P} \tag{2}$$

$$\mathrm{P} \xrightarrow[k_2]{} \mathrm{P_t} \tag{3}$$

$$\mathrm{M^*} \xrightarrow[k_3]{P} \mathrm{M} \tag{4}$$

$$\mathrm{M} \xrightarrow[k_4]{} \mathrm{M^*} \tag{5}$$

$$\mathrm{A} \xrightarrow[v_{dA}]{M} \mathrm{A_d} \tag{6}$$

$$\mathrm{P} \xrightarrow[v_{dP}]{M} \mathrm{P_t} + \mathrm{P_{t,d}} \tag{7}$$

$$\mathrm{M} \xrightarrow[v_{dM}]{M} \mathrm{M^*} + \mathrm{M_d^*} \tag{8}$$

Based on (1)-(8) for the *normal condition* case mass balances lead to the following set of differential equations:

$$\frac{dA}{dt} = v_A P_t - \frac{v_{dA} M A}{K_{mdA} + A} \tag{9}$$

$$\frac{dP}{dt} = \frac{k_1 A P_t}{K_{m1} + P_t} - \frac{k_2 P}{K_{m2} + P} - v_{dP} M P \tag{10}$$

$$\frac{dP_t}{dt} = -\frac{k_1 A P_t}{K_{m1} + P_t} + \frac{k_2 P}{K_{m2} + P} + v_{dP} M P \tag{11}$$

$$\frac{dM}{dt} = \frac{k_3 P M^*}{K_{m3} + M^*} - \frac{k_4 M}{K_{m4} + M} - v_{dM} M^2 \tag{12}$$

$$\frac{dM^*}{dt} = -\frac{k_3 P M^*}{K_{m3} + M^*} + \frac{k_4 M}{K_{m4} + M} + v_{dM} M^2 \tag{13}$$

$$\frac{dA_d}{dt} = \frac{v_{dA} M A}{K_{mdA} + A} \tag{14}$$

$$\frac{dP_{t,d}}{dt} = v_{dP} M P \tag{15}$$

$$\frac{dM_d^*}{dt} = v_{dM} M^2 \tag{16}$$

From (10) and (11), or (12) and (13), respectively, it is obvious, that the total amount of $P + P_t$ and the total amount of $M + M^*$ are constant in the normal condition case. For the total amount of $P_t + P < P_{tot}$ we consider the system as being in the $P + P_t$ *deficit* state (Fig.4). In this state, it is assumed that the cell does not produce $P_{t,d}$ for the daughter cell, but instead replenishes its own stock of $P$ and $P_t$. Then (7) is replaced by:

$$\mathrm{P} \xrightarrow[v_{dP}]{M} 2\,\mathrm{P_t} \tag{17}$$

(11) and (15) are replaced by:

$$\frac{dP_t}{dt} = -\frac{k_1 A P_t}{K_{m1} + P_t} + \frac{k_2 P}{K_{m2} + P} + 2 v_{dP} M P \tag{18}$$

$$\frac{dP_{t,d}}{dt} = 0.0 \tag{19}$$

For the case of membrane building blocks deficit (Fig.4 $M + M^*$ *deficit*) we use the following equation instead of (8):

$$\mathrm{M} \xrightarrow[v_{dM}]{M} 2\,\mathrm{M^*} \tag{20}$$

This modifies (13) and (16) in the following way:

$$\frac{dM^*}{dt} = -\frac{k_3 P M^*}{K_{m3} + M^*} + \frac{k_4 M}{K_{m4} + M} + 2 v_{dM} M^2 \tag{21}$$

$$\frac{dM_d^*}{dt} = 0.0 \tag{22}$$

The artificial cell model is solved with the parameter set listed in Table1.

Table 1. Initial conditions and parameter set.

| Initial condition/parameter | Value |
|---|---|
| $A_0$ | 0.5 |
| $P_{t_0}$, $M_0^*$ | 2.0 |
| $P_0$, $M_0$, $A_{d_0}$, $P_{t,d_0}$, $M_{d_0}^*$ | 0.0 |
| $P_{tot}$, $M_{tot}$ | 2.0 |
| $v_A$ | 0.025 |
| $K_{m_{dA}}$ | 0.002 |
| $K_{m_1}, K_{m_2}, K_{m_3}, K_{m_4}$ | 0.001 |
| $k_1$ | 3.0 |
| $k_2$ | 1.5 |
| $k_3$ | 1.0 |
| $k_4$ | 0.5 |
| $v_{dA}, v_{dP}, v_{dM}$ | 0.02 |

The system is implemented in ProMoT/DIANA (Ginkel et al. (2003); Mangold et al. (2014)).

### *2.2 Results*

By using *normal conditions* (Table 1), i. e. $P_t + P = P_{tot}$ and $M^* + M = M_{tot}$, the system shows an autonomous oscillatory behavior with a stable limit cycle (Fig.5).

The growing polymer $P$ increases when the activity of metabolism $A$ increases, and only then the catalytically active membrane building blocks $M$ increase as well. At high values of $M$ the levels of $A$ and $P$ begin to decrease caused by conversion into daughter cell components catalyzed by $M$. The catalytic activity of $M$ decreases during the degradation of the components $A_d$, $P_{t,d}$ and $M_d^*$, i. e. during the separation of the daughter cell. As soon as the replicated polymer is split catalyzed by $M$ the metabolism becomes active again and a new cycle starts.

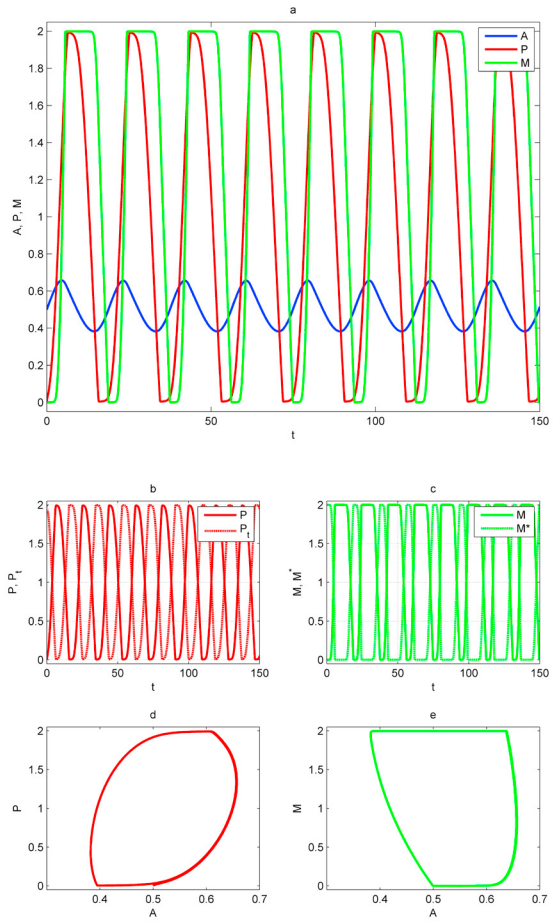


Fig. 5. Simulation results of the mother cell components. Dynamic behavior of mother cell components $A$, $P$, $M$ (a); corresponding parts of the polymerization subsystem $P$, $P_t$ (b); inactive $M^*$ and active membrane building blocks $M$ (c); stable limit cycles (d,e).

### *2.3 Self-reproduction*

To test the system with regard to the self-reproduction we look at the degraded daughter cell components. We consider the mother cell as being able of self-reproduction if the degraded amounts of $A_d$, $P_{t,d}$, $M_d^*$ at the time point of daughter cell separation are sufficient to start a new cell cycle. It is assumed that the cell division occurs, when the amount of $M$ falls below a certain threshold due to its inactivation during the separation of the daughter cell at a time point $t_{div}$. We determine the amounts of $A_d$, $P_{t,d}$, $M_d^*$ at the time point of the first separation $t_{div} = 16.6s$ and define them as the initial conditions of the daughter cell cycle (Table 2).

Table 2. Initial conditions for the daughter cell cycle determined from degraded materials $A_d$, $P_{t,d}$, $M_d^*$ at time point $t_{div} = 16.6s$.

| Initial condition | Value |
|---|---|
| $A_{d_0}$ | 0.4629 |
| $P_{d_0}$ | 0.0 |
| $P_{t,d_0}$ | 0.6275 |
| $M_{d_0}$ | 0.0 |
| $M^*_{d_0}$ | 0.8671 |

The self-reproduction study shows that the quantities of conversed materials are sufficient to initiate a new cell cycle of daughter cell after a certain phase of adaptation to new conditions (Fig.6). Based on the determined initial conditions for the daughter cell we have the case of $P_d + P_{t,d}$ *deficit* and $M_d + M_d^*$ *deficit*, as a result of which the polymerization subsystem proliferates firstly until the condition $P_d + P_{t,d} = P_{tot}$ is reached. Then the system merges to the proliferation of the membrane subsystem until it achieves the condition $M_d + M_d^* = M_{tot}$. Only then the case of *normal condition* persists about after $200s$ and we can see the same dynamic behavior of the daughter cell as of the mother cell. Consequently, the model offers a robust self-replicating state.

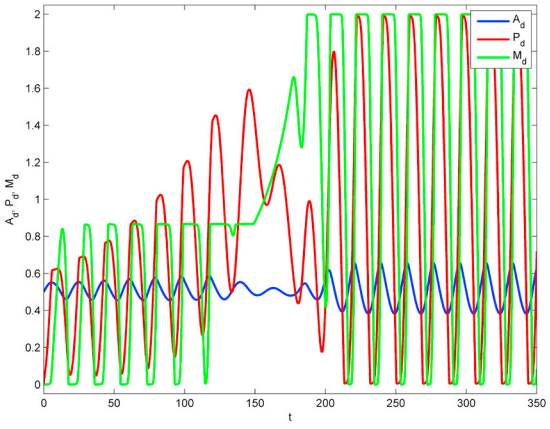


Fig. 6. Dynamic behavior of daughter cell's metabolism $A_d$, growing polymer $P_d$ and catalytically active membrane building blocks $M_d$ in the *deficit* case.

### *2.4 Robustness with respect to parameter changes*

In addition to self-reproduction we can show that the model is robust with respect to parameter uncertainties. By changing the parameters by about ±20% compared to the case of *normal condition* the system indicates the same oscillating behavior (Fig.7). It is obvious that for parameter changes of −20% the period of the cycle is extended while for a +20% increase of the parameter values, the period becomes shorter, i.e. the cell divides faster.

## 3. CONSIDERATION OF VOLUME CHANGES

So far, we have assumed that the cell volume is constant throughout the complete cell cycle. However, in reality the protocell's volume will increase with its mass. To account for this effect, dilution terms $\frac{A}{V}\frac{dV}{dt}$, $\frac{P}{V}\frac{dV}{dt}$, $\frac{M}{V}\frac{dV}{dt}$ are added to the model equations in the following. We assume that the volume changes are proportional to the change of the membrane building blocks $M$ caused by insertion of the newly generated membrane building blocks $M$ into the membrane. We consider the case of *normal condition*, so we examine the system of three differential equations (23)-(25) by assuming $P_t = P_{tot} - P$, $M^* = M_{tot} - M$ and by using (26), (27).

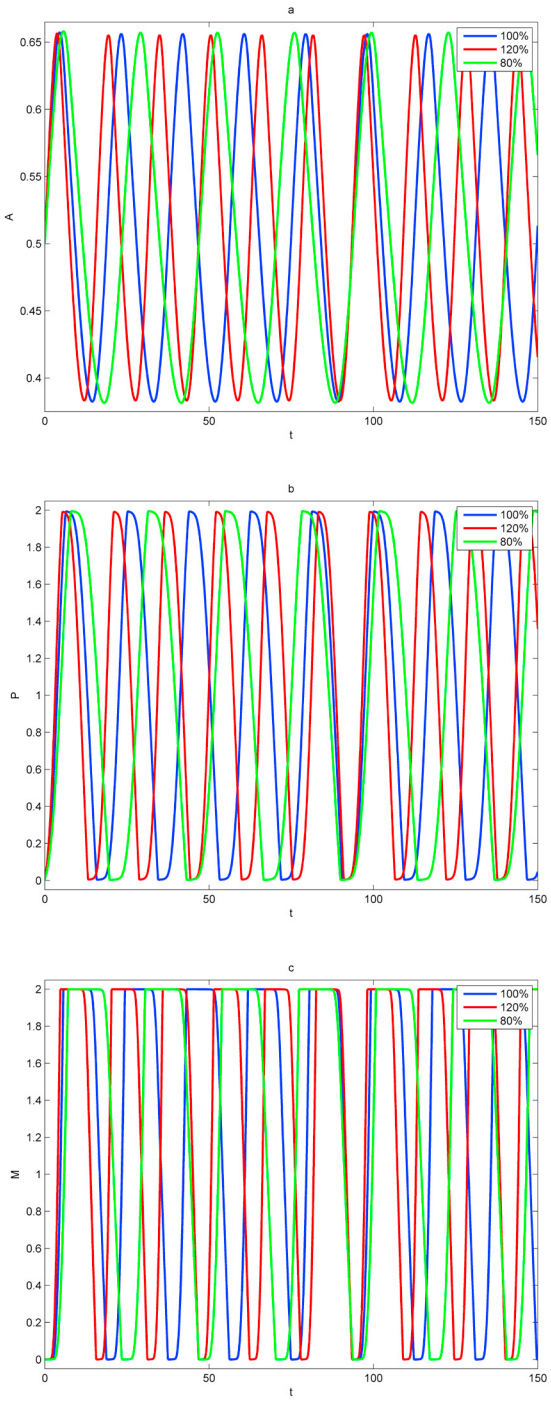


Fig. 7. Parameter uncertainties study by changing the parameters by about ±20%. Parameter changes with respect to metabolist $A$ (a), growing polymer $P$ (b), active membrane building blocks $M$ (c).

$$\frac{dA}{dt} = v_A(P_{tot} - P) - \frac{v_{dA} M A}{K_{mdA} + A} - \frac{A}{V}\frac{dV}{dt} \tag{23}$$

$$\frac{dP}{dt} = \frac{k_1 A(P_{tot} - P)}{K_{m1} + (P_{tot} - P)} - \frac{k_2 P}{K_{m2} + P} - v_{dP} M P - \frac{P}{V}\frac{dV}{dt} \tag{24}$$

$$\frac{dM}{dt} = \frac{k_3 P(M_{tot} - M)}{K_{m3} + (M_{tot} - M)} - \frac{k_4 M}{K_{m4} + M} - v_{dM} M^2 - \frac{M}{V}\frac{dV}{dt} \tag{25}$$

The volume $V$ is determined from the affine equation (28). Thereby the factor $\sigma$ defines the space captured by one membrane molecule $M$.

$$\frac{1}{V}\frac{dV}{dt} = \frac{V_0 \sigma r_M}{V + V_0 \sigma M} \tag{26}$$

$$r_M = \frac{k_3 P(M_{tot} - M)}{K_{m3} + (M_{tot} - M)} - \frac{k_4 M}{K_{m4} + M} - v_{dM} M^2 \tag{27}$$

$$V = V_0 + V_0 \sigma M \tag{28}$$

The initial conditions and parameter set for the implementation of the volume expansion model are listed in Table 3.

Table 3. Initial conditions and parameter set for the model including volume expansion.

| Initial condition/parameter | Value |
|---|---|
| $A_0$ | 0.1402 |
| $P_0$ | 0.1181 |
| $M_0$ | 0.1609 |
| $V_0$ | 100.0 |
| $v_A$ | 0.025 |
| $K_{m_{dA}}$ | 0.00002 |
| $K_{m_1}, K_{m_2}$ | 0.001 |
| $K_{m_3}, K_{m_4}$ | 0.00011 |
| $k_1$ | 4.5 |
| $k_2$ | 0.395 |
| $k_3, k_4$ | 0.6 |
| $v_{dA}$ | 0.02 |
| $v_{dP}, v_{dM}$ | 0.002 |
| $\sigma$ | 0.5 |

The extended system shows stable periodic oscillations in the intracellular components of the mother cell in spite of the dilution due to the volume increase (Fig.8). At the maximal concentration of membrane building blocks $M$ the volume reaches the maximal value as well, and it decreases during the separation of the daughter cell, when $M$ decreases. An adjustment of the parameters compared to section 2 is needed, because the region of existence of periodic solutions is shifted in the extended model. The parameter adjustment causes a shorter cell cycle time compared to the model without volume expansion. However, periodic solutions still occur for wide parameter ranges (Fig.9). This means that the property of robustness is preserved in the extended model.

## 4. CONCLUSION

The model shown in this work describes an artificial self-reproducible cell cycle, which is robust with respect to parameter uncertainties. Furthermore we considered the synchronization problem of intracellular changes with the volume expansion. It is found that the synchronization inside the cell is strongly dependent on the parameter set and the space proportionality factor $\sigma$.

A further question, that we want to study in the future, is how the Chemoton model of T. Gánti (Gánti, 2003) can be

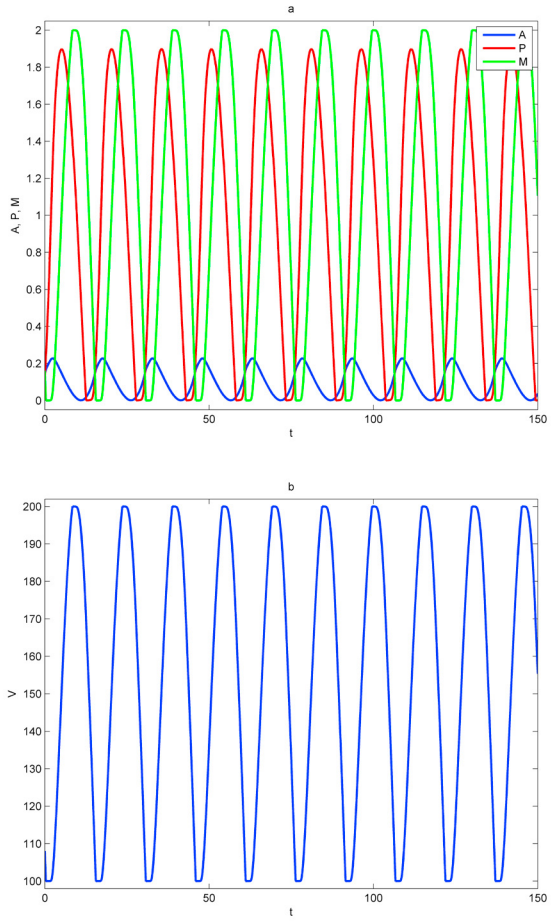


Fig. 8. Simulation results of the model taking into account of volume changes. Dynamic behavior of mother cell devices: metabolism $A$, growing polymer $P$, newly generated catalytically active membrane building blocks $M$ (a). Volume changes (b).

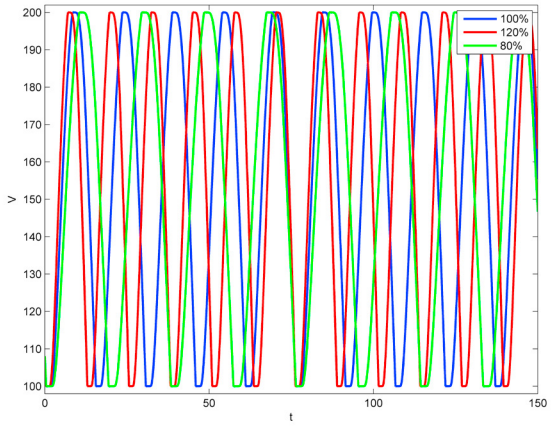


Fig. 9. Volume changes of the extended model with respect to parameter changes by about ±20%.

modified and reduced to accomplish similar synchronization of the concentration changes with the volume change as the model described in this work. In addition we want to expand the model described here with respect to the polymerization subsystem similar to the Chemoton. In this way we expect to gradually approach these two models in order to better understand the synchronization mechanism of the Chemoton model.

## REFERENCES

Csendes, T. (1984). A simulation study on the chemoton. *Kybernetes*, 13(2), 79–85.

Gánti, T. (2003). *Chemoton theory*, volume 1: Theoretical foundations of fluid machineries, 144–159. Kluwer Academic/Plenum Publishers.

Ginkel, M., Kremling, A., Nutsch, T., Rehner, R., and Gilles, E.D. (2003). Modular modeling of cellular systems with ProMoT/diva. *Bioinformatics*, 19(9), 1169–1176. doi:10.1093/bioinformatics/btg128.

Goldbeter, A. (1991). A minimal cascade model for the mitotic oscillator involving cyclin and cdc2 kinase. *Proceedings of the National Academy of Sciences*, 88(20), 9107–9111. doi:10.1073/pnas.88.20.9107.

Jaschke, P.R., Lieberman, E.K., Rodriguez, J., Sierra, A., and Endy, D. (2012). A fully decompressed synthetic bacteriophage X174 genome assembled and archived in yeast. *Virology*, 434(2), 278–284. doi:10.1016/j.virol.2012.09.020.

Keasling, J.D. (2012). Synthetic biology and the development of tools for metabolic engineering. *Metabolic Engineering*, 14(3), 189–195. doi:10.1016/j.ymben.2012.01.004.

Mangold, M., Khlopov, D., Danker, G., Palis, S., Svjatnyj, V., and Kienle, A. (2014). Development and nonlinear analysis of dynamic plant models in ProMoT/diana. *Chemie Ingenieur Technik*, 86(7), 1107–1116. doi:10.1002/cite.201400003.

Novák, B. and Tyson, J.J. (2008). Design principles of biochemical oscillators. *Nature Reviews Molecular Cell Biology*, 9(12), 981–991. doi:10.1038/nrm2530.

Pohorille, A. and Deamer, D. (2002). Artificial cells: prospects for biotechnology. *Trends in Biotechnology*, 20(3), 123–128. doi:10.1016/S0167-7799(02)01909-1.

Rasmussen, S., Chen, L., Nilsson, M., and Abe, S. (2003). Bridging nonliving and living matter. *Artificial Life*, 9(3), 269–316. doi:10.1162/106454603322392479.

Stano, P. (2011). Advances in minimal cell models: a new approach to synthetic biology and origin of life. In A. Carpi (ed.), *Progress in Molecular and Environmental Bioengineering - From Analysis and Modeling to Technology Applications*. InTech.